Journal of Alloys and Compounds 509 (2011) 3958–3962

Contents lists available at ScienceDirect

Journal of Alloys and Compounds

journal homepage: www.elsevier.com/locate/jallcom

Preparation and electrical properties of $Bi_{0.5}Na_{0.5}TiO_3$–$BaTiO_3$–$KNbO_3$ lead-free piezoelectric ceramics

Haimin Ni[a], Laihui Luo[a,*], Weiping Li[a], Yuejin Zhu[a,*], Haosu Luo[b]

[a] Department of Physics, Ningbo University, Ningbo 315211, China
[b] Shanghai Institute of Ceramics, Chinese Academy of Sciences, Shanghai 20050, China

ARTICLE INFO

Article history:
Received 22 September 2010
Accepted 28 December 2010
Available online 4 January 2011

Keywords:
Lead-free ceramic
Piezoelectric
Ferroelectric
Dielectric

ABSTRACT

Lead-free $(1-x)Bi_{0.47}Na_{0.47}Ba_{0.06}TiO_3$–$xKNbO_3$ (BNBT–xKN, x = 0–0.08) ceramics were prepared by ordinary ceramic sintering technique. The piezoelectric, dielectric and ferroelectric properties of the ceramics are investigated and discussed. The results of X-ray diffraction (XRD) indicate that $KNbO_3$ (KN) has diffused into $Bi_{0.47}Na_{0.47}Ba_{0.06}TiO_3$ (BNBT) lattices to form a solid solution with a pure perovskite structure. Moderate additive of KN ($x \le 0.02$) in BNBT–xKN ceramics enhance their piezoelectric and ferroelectric properties. Three dielectric anomaly peaks are observed in BNBT–0.00KN, BNBT–0.01KN and BNBT–0.02KN ceramics. With the increment of KN in BNBT–xKN ceramics, the dielectric anomaly peaks shift to lower temperature. BNBT–0.01KN ceramic exhibits excellent piezoelectric properties and strong ferroelectricity: piezoelectric coefficient, d_{33} = 195 pC/N; electromechanical coupling factor, k_t = 58.9 and k_p = 29.3%; mechanical quality factor, Q_m = 113; remnant polarization, P_r = 41.8 μC/cm^2; coercive field, E_c = 19.5 kV/cm.

Published by Elsevier B.V.

1. Introduction

Currently, lead zirconate titanate (PZT) and PZT-based multi-component systems dominate piezoelectric ceramic applications because of their excellent electrical properties near the morphotropic phase boundary (MPB). However, the use of lead-based piezoelectric ceramics has caused serious lead pollution due to the high toxicity of lead oxide and its high volatility during sintering. Therefore, much attention has been paid to the development of lead-free piezoelectric ceramics with good piezoelectric properties.

Sodium bismuth titanate, $Bi_{0.5}Na_{0.5}TiO_3$ (BNT), is considered to be one of the promising candidates as lead-free piezoelectric ceramics due to its large remnant polarization at room temperature. BNT exhibits a remnant polarization (P_r) of 38 μC/cm^2 and a coercive field (E_c) of 73 kV/cm [1]. However, the poling of the BNT is very difficult due to its high E_c, which lead to the low piezoelectric property of BNT ceramic. To improve the piezoelectric performance of BNT, lots of other lead-free piezoelectric components have been added to BNT to form BNT-based solid solutions, such as BNT–$Bi_{0.5}K_{0.5}TiO_3$ [2,3], BNT–$BaTiO_3$ [4–7], BNT–$KNbO_3$ [8,9], BNT–$NaNbO_3$ [8,10], BNT–$Bi_{0.5}K_{0.5}TiO_3$–$Bi_{0.5}Li_{0.5}TiO_3$ [11,12], BNT–$Bi_{0.5}K_{0.5}TiO_3$–$BaTiO_3$ [13,14] and BNT–$BaTiO_3$–$KNaNbO_3$ [15,16], have been studied extensively. $KNbO_3$ (KN) is also a good candidate of lead-free piezoelectric material due to its high Curie temperature (T_c = 435 °C) and large spontaneous polarization (P_s = 30 μC/cm^2) [9]. On the other hand, there is MPB in the multi-component BNT-based solid solutions, and the solid solutions exhibit large piezoelectric properties near MPB. Consequently, research activities have been mainly focused on the MPB region of solid solution systems. The MPB of $(1-x)$BNT–$x$$BaTiO_3$ locates at x = 0.06–0.07 [17,18], and the MPB of $(1-x)$BNT–$x$$KNbO_3$ resides at x = 0.04–0.06 [9]. Therefore, there should be MPB in the ternary system $Bi_{0.5}Na_{0.5}TiO_3$–$BaTiO_3$–$KNbO_3$. For lead-based ceramics, it has been known that multi-component ceramics usually possess better piezoelectric performances than single or binary-component ceramics because of the formation of the more complex MPB [12]. Therefore, the research and development of new lead-free ceramics should be put on designing new multi-component piezoelectric ceramics near their MPB. According the rules mentioned as above, a new ternary system BNT-based lead-free ceramic, $Bi_{0.5}Na_{0.5}TiO_3$–$BaTiO_3$–$KNbO_3$, is developed in this work. In this ternary system, the mole ratio of $Bi_{0.5}Na_{0.5}TiO_3/BaTiO_3$ is constant 0.94/0.06. The chemical formula of ternary system ceramic is written as $(1-x)Bi_{0.47}Na_{0.47}Ba_{0.06}TiO_3$–$xKNbO_3$ (BNBT–xKN, x = 0–0.08). In the present work, BNBT–xKN ceramics were prepared by a conventional solid-state sintering processing, and their microstructures, dielectric, ferroelectric and piezoelectric were studied systematically.

---

* Corresponding authors. Tel.: +86 574 87600953; fax: +86 574 87600744.
E-mail address: llhsic@126.com (L. Luo).

0925-8388/$ – see front matter. Published by Elsevier B.V.
doi:10.1016/j.jallcom.2010.12.190

2. Experimental

BNBT–xKN lead-free ceramics were prepared by a conventional ceramic fabrication process. $Bi_{0.47}Na_{0.47}Ba_{0.06}TiO_3$ (BNBT) and $KNbO_3$ (KN) powders were prepared in advance. Analytical-grade powders: Bi_2O_3 (99.9%), Na_2CO_3 (99.8%), $BaCO_3$ (99%), TiO_2 (99%), K_2CO_3 (99%) and Nb_2O_5 (99.5%) were used as starting powders to synthesize BNBT and KN powders, respectively. The powders in the stoichiometric ratio were mixed and milled thoroughly in alcohol using agate balls for 10 h, and then dried and calcined at 850 °C for 2 h. The synthesized BNBT and KN powders were weighted according to chemical formula BNBT–xKN (x = 0–0.08). The BNBT and KN powders were mixed and milled again for 10 h. After drying, the powders were sieved and mixed thoroughly with a PVA binder solution, and then pressed into disk samples with a pressure of ~100 MPa. The disk samples were then sintered at 1150 °C for 2 h in air. Silver paste was pasted on the top and bottom surfaces of the disc samples and then fired at 650 °C. All the samples were poled under a dc field of 5 kV/mm at 85 °C in a silicon oil bath for 20 min, and then cooled to room temperature under the poling field. The crystal structure of the sintered samples was measured using X-ray diffraction (XRD) analyzer (Bruker D8 Advance) with Cu Kα radiation. The dielectric constant ε_{33} and dielectric loss tan δ of the ceramics as a function of temperature at 100 Hz, 1 kHz, 10 kHz, 100 kHz and 1 MHz were measured using an impedance analyzer (Agilent 4294A). The polarization vs. electric field (P–E) hysteresis loop was carried out at 1 Hz with the RT Premier II ferroelectric workstation. The electromechanical coupling factor k_p, k_t and mechanical quality factor Q_m were calculated using the resonance method according to the IEEE Standard 176 with the impedance analyzer Agilent 4294A. The piezoelectric strain coefficient d_{33} was measured by a quasistatic piezoelectric meter (ZJ-3AN, China).

3. Results and discussions

The XRD patterns of the BNBT–xKN ceramics are shown in Fig. 1(a), which indicates that all the samples have a single-phase perovskite structure and KN has diffused into the lattices to form a solid solution. The peaks of the BNBT–xKN ceramics shift to lower 2θ angel as the KN content increases in BNBT–xKN ceramics, which indicate an increment in lattice constant as a function of the KN content. Fig. 1(b) is the XRD patterns in Fig. 1(a) with the 2θ angel ranging from 45° to 48°. Only the (2 0 0) peak is observed for all the BNBT–xKN ceramics. As we know, $Bi_{0.47}Na_{0.47}Ba_{0.06}TiO_3$ locates at MPB of the rhombohedral and the tetragonal phases [1,17,18]. On the other hand, potassium niobate KN [19] is orthorhombic at −10 to 225 °C. The peak (2 0 0) in Fig. 1(b) does not separate with the increment of KN, which indicates that no phase transition occurs from rhombohedral to tetragonal or other phase with the increment of KN in BNBT–xKN ceramics.

Fig. 2 exhibits the P–E hysteresis loops of BNBT–xKN samples. The loop of BNBT–0.00KN ceramic is well saturated and square-like, as shown in Fig. 2(a). The coercive field (E_c) and remnant polarization (P_r) of BNBT–0.00KN reach 27.5 kV/cm and 33.1 μC/cm^2, respectively. From Fig. 2, it is shown that P_r increases with the increment of x and then decreases at $x > 0.02$, exhibiting a maximum value at $x = 0.01$. E_c decreases with x ($x \leqq 0.02$), and than increase with x ($x \geqq 0.04$). It is obvious that E_c reduces and P_r increases greatly for the introduction of moderate KN into BNBT ceramics. However, the excess additive of KN weakens the ferroelectric properties of BNBT–xKN ceramics. For BNBT–0.01KN and BNBT–0.02KN, the P–E loops become slimmer, compared with that of BNBT–0.00KN ceramic. The E_c and P_r of BNBT–0.01KN are 19.5 kV/cm and 41.8 μC/cm^2, respectively, and P_r is much larger than that of BNBT–0.00KN ceramic. The P–E hysteresis loops of BNBT–0.01KN and BNBT–0.02KN are deformed, which are similar with double hysteresis loop of antiferroelectrics to some extent. The deformed hysteresis loop is attributed the phase transition induced by electric field. The polarization is difficult to saturate as x increases due to its leakage at high electric field. The ferroelectric characteristics of the BNBT–xKN samples become weak when x increases to x = 0.04, 0.08, and the hysteresis loops become less saturated. E_c of BNBT–0.08KN reaches 25.5 kV/cm; meanwhile, P_r is only 18.5 μC/cm^2. The less saturated hysteresis loops and the weaker ferroelectricity of the BNBT–xKN ceramics with $x > 0.04$ may be attributed to two reasons: (i) possible occurrence of non-polar regions induced by the substitution of K^{1+} for A site and Nb^{5+} for B site in ABO_3 perovskite ferroelectrics in BNBT–xKN ceramics at room temperature. A similar result has been reported in $(Bi_{0.5}Na_{0.5})_{0.94}Ba_{0.06}Zr_yTi_{1-y}O_3$ and $(Bi_{0.94-x}La_xNa_{0.94})_{0.5}Ba_{0.06}TiO_3$ ceramics, in which the additive leads to the existence of non-polar regions [20,21]; (ii) high lever of additive will generate many defects due to charge compensation, and the defects will move at high electric field, which leads to the difficulty of saturated polarization at high field due to the leakage. Moderate content of additive KN enhances the phase transition between rhombohedra and tetragonal phase in MPB, which induces a high piezoelectric effect.

The dielectric constant ε_{33} and dielectric loss tan δ of the poled samples as a function of temperature are measured with frequencies 100 Hz, 1 kHz, 10 kHz, 100 kHz and 1 MHz, which are shown as Fig. 3. From Fig. 3(a)–(c), the three samples with different KN content (x = 0.00, 0.01, 0.02) exhibit three obvious dielectric anomaly peaks. The first dielectric anomaly peak occurs at the depolarization temperature T_d. When BNBT–xKN ceramics are heated to the temperature above T_d, the piezoelectric effect of the samples disappears. T_d can be obtained from the temperature of tan δ's first peak. It is a diffusion phase transition at T_d because of the variety of T_d with test frequency. The second dielectric anomaly peak appears at temperature T_s. This dielectric anomaly might be responsible for the defects generated during sintering due to the high evaporation of Bi, Na and K during sintering. The second dielectric anomaly disappears when the test frequency increases to 1 MHz. While T_m responds to the temperature at which dielectric constant ε_{33} obtains the maximum value. For the curve of BNBT–0.00KN ceramic at 1 kHz, the T_d and T_m is 105 and 297 °C, respectively. T_d and T_m decrease as KN content increases in BNBT–xKN. When x increases to 0.04, T_d is not observed at above room temperature. It is likely that T_d has moved to lower temperature than room temperature. T_m observed in Fig. 3 is nearly independent on the test frequency. However, T_d depends on the measurement frequency; which indicates that it is a diffuse phase transition. The researchers have different opinions on the depolarization temperature T_d. Many researchers consider that phase transition from a ferroelectric phase to the so-called 'anti-ferroelectric' phase occurs at T_d in BNT-based lead-free piezoelectric ceramics due to the appearance of 'double' hysteresis loop near T_d [8,10–16]. However, experiment such as X-ray diffraction, Raman and neutron scattering does not support the existence of anti-ferroelectric phase above T_d in BNT-based ceramic [22–24]. If the ferroelectric to anti-ferroelectric phase transition occurs at T_d in NBT-based ceramics, the anti-ferroelectric phase should exist in the whole temperature range between T_d and T_m. However, the 'double' hysteresis loop appears not in the whole temperature range between T_d and T_m. For the BNT-based ceramics, it appears even below T_d [9,12,21]. While, some researchers consider that macro–micro domain switching occurs at T_d in BNT-based ceramics [9,17]. Heat destroys the macro-domain state, the ferroelectrics stay in macro-domain state at temperature below T_d, and macro-domain state transforms to micro-domain state at temperature above T_d [25]. The macro–micro domain switching leads to the changing of electrical properties of the ferroelectrics, occurring of depolarization and so on. Furthermore, the strong electric field can lead to the micro-domain state transform to macro-domain state, which can result in the appearance of the 'double' hysteresis loop. Macro–micro domain switching could be used to explain the dielectric anomaly peak at depolarization temperature T_d in BNBT–xKN ceramics. There are micro-domains in poled BNBT–0.01KN and BNBT–0.02KN ceramics below T_d due to composition fluctuation and disorder of 'A' site in BNBT–xKN. The

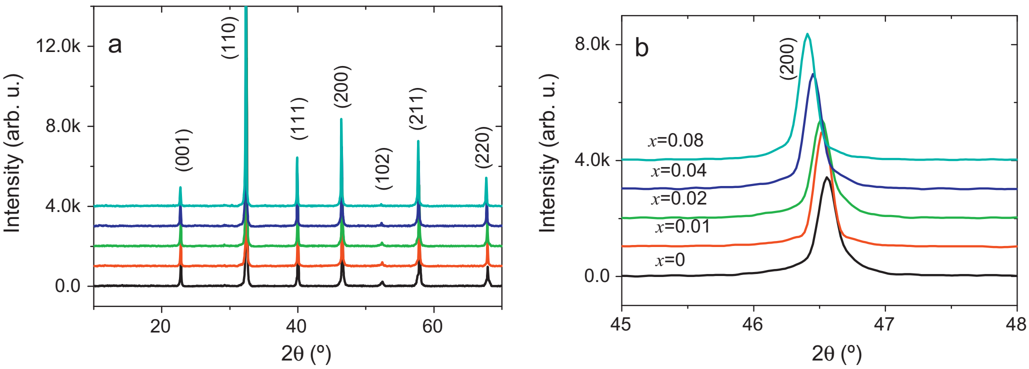

Fig. 1. XRD patterns of BNBT–xKN ceramics.

hysteresis loops deform due to the micro–macro domain switching induced by electric field, which is similar with the loop of anti-ferroelectrics to some extent. At room temperature, BNBT–0.04KN and BNBT–0.08KN ceramics stay in micro-domain state due to their lower T_d, and the electric field is not enough to induce the transformation from micro-domain state to macro-domain state. So the 'double' hysteresis loop is not observed in BNBT–0.04KN and BNBT–0.08KN ceramics.

Fig. 4(a) exhibits the piezoelectric coefficient d_{33} and the electromechanical coupling factor k_t of BNBT–xKN ceramics as a function of KN mole content. d_{33} and k_t achieve the maximum value of $d_{33} = 195$ pC/N and $k_t = 58.9\%$ at $x = 0.01$. d_{33} and k_t reduce

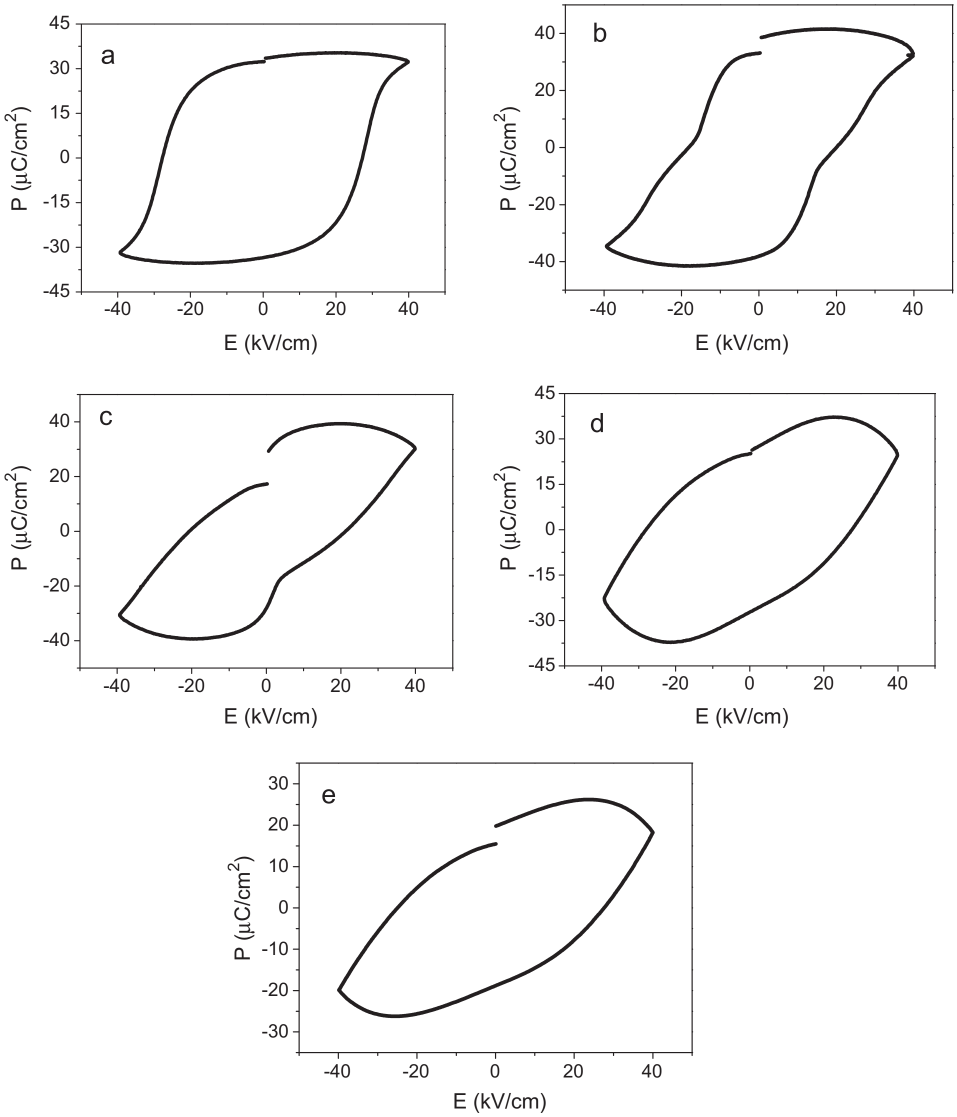

Fig. 2. Polarization vs. electric field hysteresis loops of BNBT–xKN ceramics: (a) $x = 0.00$, (b) $x = 0.01$, (c) $x = 0.02$, (d) $x = 0.04$, (e) $x = 0.08$.

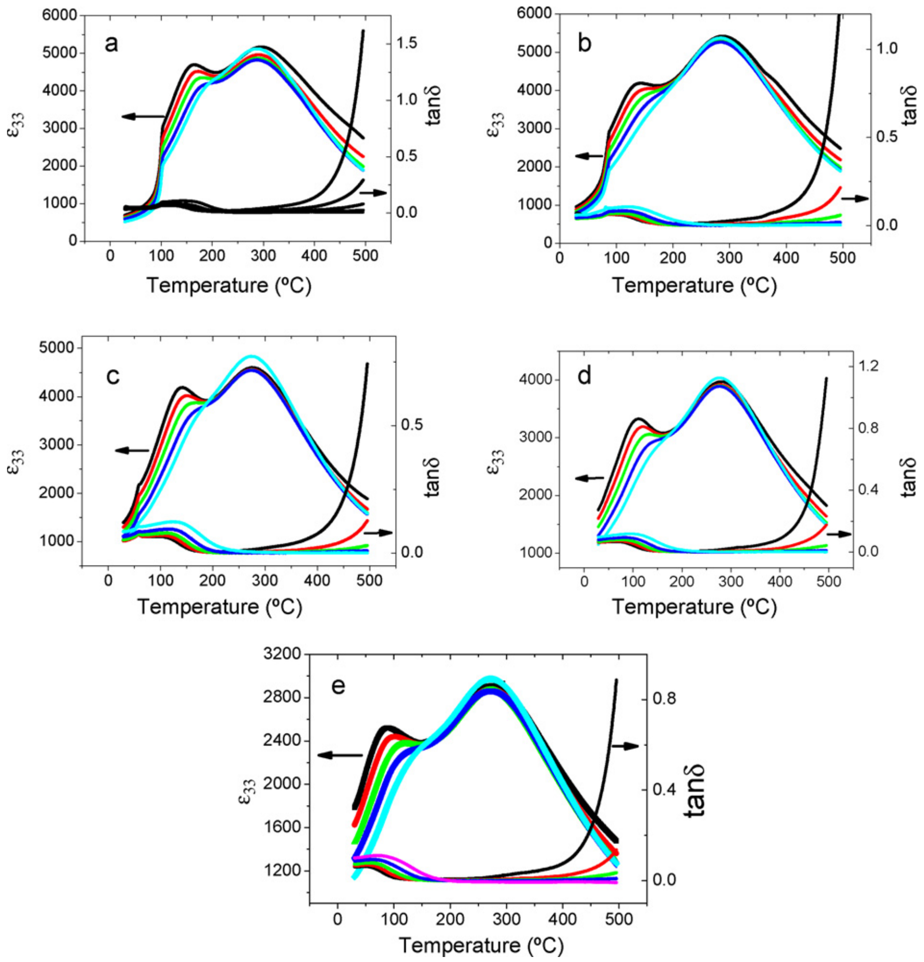

Fig. 3. Dielectric constant ε_{33} and dielectric loss tan δ of the BNBT–xKN ceramics as a function of temperature measured with frequencies 100 Hz, 1 kHz, 10 kHz, 100 kHz and 1 MHz: (a) $x = 0.00$, (b) $x = 0.01$, (c) $x = 0.02$, (d) $x = 0.04$, (e) $x = 0.08$.

greatly when KN content $x > 0.02$. BNBT–0.04KN and BNBT–0.08KN ceramics exhibit a much lower d_{33} value, their d_{33} values are 9 and 4 pC/N, separately, which is near zero. Their small piezoelectric values are attributed to their micro-structure. T_d of BNBT–0.04KN and BNBT–0.08KN ceramics is lower than room temperature, so the domain structure of BNBT–0.04KN and BNBT–0.08KN ceramics is micro-domain at room temperature. The micro-domain leads to the low piezoelectric effect. Fig. 4(b) shows the dielectric constant ε_{33} and dielectric loss tanδ measured at 1 kHz for BNBT–xKN ceramics. The behaviors of ε_{33} and tanδ as a function of KN mole content are similar. ε_{33} and tan δ increase sharply with KN mole content, and than increase moderately. Fig. 5 shows the planar electromechanical coupling factor k_p and mechanical quality factor Q_m of BNBT–xKN ceramics. The figure shows that k_p decreases with KN content. k_p of BNBT–0.01KN ceramic is 29.3%. Mechanical quality factor Q_m of the ceramics first reduces with KN content, and then increases with KN content when x over 0.02.

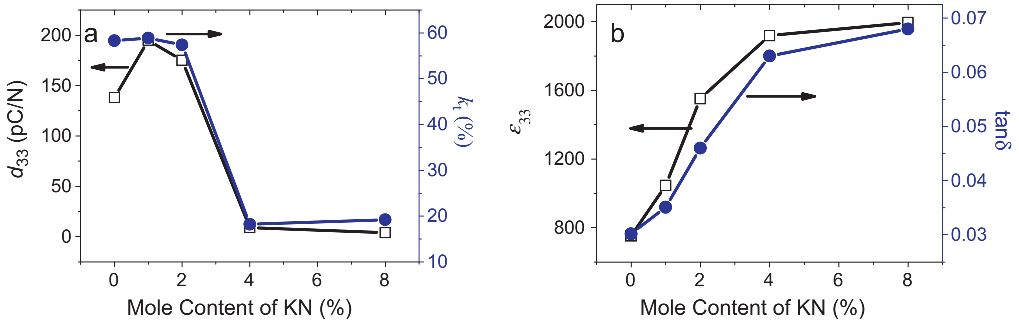

Fig. 4. (a) Piezoelectric coefficient d_{33} and the electromechanical coupling factor k_t of BNBT–xKN ceramics as a function of KN mole content, (b) dielectric constant ε_{33} and dielectric loss tan δ of BNBT–xKN ceramics at 1 kHz.

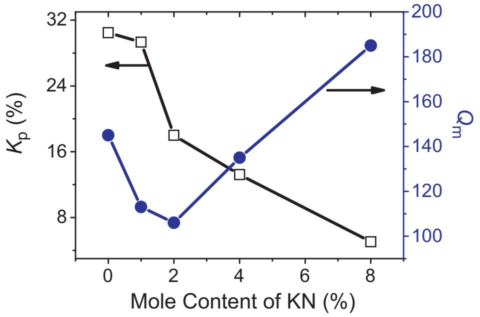

Fig. 5. Planar electromechanical coupling factor k_p and mechanical quality factor Q_m of BNBT–*x*KN ceramics.

4. Conclusion

A novel ternary lead-free piezoelectric ceramic BNBT–*x*KN is developed in this paper. BNBT–*x*KN ceramics have been prepared by a conventional ceramic sintering technique and their piezoelectric, ferroelectric and dielectric performances have been investigated. The results of XRD indicate that KN has diffused into the BNBT lattices to form a new solid solution with a pure perovskite structure, no phase transition is observed by adding KN into BNBT. Moderate introduction of KN into BNBT–*x*KN ceramic ($x \leq 0.02$) can enhance the piezoelectric, dielectric and ferroelectric properties of BNBT–*x*KN. BNBT–0.01KN ceramic exhibits best piezoelectric properties and strong ferroelectricity: piezoelectric coefficient, $d_{33} = 195$ pC/N, electromechanical coupling factor, $k_t = 58.9$ and $k_p = 29.3\%$, quality factor, $Q_m = 113$, remanent polarization, $P_r = 41.8\ \mu C/cm^2$, coercive field, $E_c = 19.5$ kV/cm. The piezoelectric properties of BNBT–*x*KN ceramics deteriorates at high level of additive of KN ($x \geq 0.04$), which is attributed to the low depolarization temperature T_d. Macro–micro domain switching occurs at T_d. T_d depends on the content of KN in BNBT–*x*KN ceramics greatly.

Acknowledgements

This work was supported by National Natural Science Foundation of China (60807036, 51002082), Natural Science Foundation of Zhejiang Province (Y4090429) Natural Science Foundation of Ningbo (2009A610103, 2009A610056), Scientific Research Fund of Zhejiang Provincial Education Department (Y200803542, Y200804227), and K.C. Wong Magna Foundation in Ningbo University (xkl09063).

References

[1] T. Takenaka, K. Maruyama, K. Sakata, Jpn. J. Appl. Phys. 30B (1991) 2236.
[2] I. Makoto, Y. Katsuya, S. Muneyasu, N. Yuji, M. Masaru, Appl. Phys. Lett. 93 (2008) 242903.
[3] A. Sasaki, T. Chiba, Y. Mamiya, E. Otsuki, Jpn. J. Appl. Phys. 38 (1999) 5564.
[4] C. Xu, D. Lin, K.W. Kwok, Solid State Commun. 10 (2008) 934–940.
[5] T. Zhou, R. Huang, X. Shang, Fei Peng, et al., Appl. Phys. Lett. 90 (2007) 182903.
[6] W. Ge, H. Liu, X. Zhao, X. Pan, T. He, et al., J. Alloy Compd. 456 (2008) 503.
[7] J. Shi, W. Yang, J. Alloy Compd. 472 (2009) 267.
[8] T. Takenaka, Ferroelectrics 230 (1999) 87–98.
[9] G. Fan, W. Lu, X. Wang, F. Liang, J. Xiao, J. Phys. D: Appl. Phys. 41 (2008) 035403.
[10] Y. Li, W. Chen, J. Zhou, Q. Xu, H. Sun, R. Xu, Mat. Sci. Eng. B – Solid 112 (2004) 5–9.
[11] D. Lin, D. Xiao, J. Zhu, P. Yu, H. Yan, L. Li, Mater. Lett. 58 (2004) 615–618.
[12] D. Lin, K.W. Kwok, H.L.W. Chan, Solid State Ionics 178 (2008) 1930–1937.
[13] X.X. Wang, X.G. Tang, H.L.W. Chan, Appl. Phys. Lett. 85 (2004) 91.
[14] H. Nagata, M. Yoshida, Y. Makiuchi, T. Takenaka, Jpn. J. Appl. Phys. 42 (2003) 7401–7403.
[15] S. Zhang, B.K. Alain, J. Wook, J. Christine, S. Klaus, G. Torsten, R. Jürgen, D. Dragan, Adv. Mater. 21 (2010) 4716–4720.
[16] S. Zhang, A.B. Kounga, E. Aulbach, H. Ehrenberg, J. Rödel, Appl. Phys. Lett. 91 (2007) 112906.
[17] B. Chu, D. Chen, G. Li, Q. Yin, J. Eur. Ceram. Soc. 22 (2002) 2115–2121.
[18] R. Ranjan, A. Dviwedi, Solid State Commun. 135 (2005) 394–399.
[19] G. Shirane, H. Danner, A. Pavlovic, R. Pepinsky, Phys. Rev. 93 (1954) 672–673.
[20] Y. Yao, T. Tseng, C. Chou, H.D.C. Haydn, J. Appl. Phys. 102 (2007) 094102.
[21] Q. Zheng, C. Xu, D. Lin, Dg Gao, K.W. Kwok, J. Phys. D: Appl. Phys. 41 (2008) 125411.
[22] J.A. Zvirgzds, P.P. Kapostins, J.V. Zvirgde, T.V. Kruzina, Ferroelectrics 40 (1982) 75–77.
[23] M.S. Zhang, J.F. Scott, Ferroelectr. Lett. 6 (1986) 147–152.
[24] S.B. Vakhrushev, V.A. Isupov, B.E. Kvyatkovsky, N.M. Okuneva, I.P. Pronin, G.A. Smolensky, P.P. Syrnikov, Ferroelectrics 63 (1985) 153–160.
[25] X. Yao, Z. Chen, L.E. Cross, J. Appl. Phys. 54 (1983) 339–403.